Measurement of Polarization and Triple-Product Correlations in $B \to \phi K^*$ Decays

K.-F. Chen,[25] K. Abe,[8] K. Abe,[39] H. Aihara,[41] Y. Asano,[45] V. Aulchenko,[1] T. Aushev,[12] S. Bahinipati,[4] A. M. Bakich,[36] I. Bedny,[1] U. Bitenc,[13] I. Bizjak,[13] S. Blyth,[25] A. Bondar,[1] A. Bozek,[26] M. Bračko,[8,19,13] J. Brodzicka,[26] T. E. Browder,[7] M.-C. Chang,[25] P. Chang,[25] Y. Chao,[25] A. Chen,[23] W. T. Chen,[23] B. G. Cheon,[3] R. Chistov,[12] S.-K. Choi,[6] Y. Choi,[35] A. Chuvikov,[48] J. Dalseno,[20] M. Danilov,[12] M. Dash,[46] A. Drutskoy,[4] S. Eidelman,[1] Y. Enari,[21] F. Fang,[7] S. Fratina,[13] N. Gabyshev,[1] A. Garmash,[48] T. Gershon,[8] G. Gokhroo,[37] B. Golob,[18,13] A. Gorišek,[13] J. Haba,[8] N. C. Hastings,[41] K. Hayasaka,[21] H. Hayashii,[22] M. Hazumi,[8] L. Hinz,[17] T. Hokuue,[21] Y. Hoshi,[39] S. Hou,[23] W.-S. Hou,[25] Y. B. Hsiung,[25] T. Iijima,[21] A. Imoto,[22] K. Inami,[21] A. Ishikawa,[8] H. Ishino,[42] R. Itoh,[8] M. Iwasaki,[41] Y. Iwasaki,[8] J. H. Kang,[47] J. S. Kang,[15] P. Kapusta,[26] N. Katayama,[8] H. Kawai,[2] T. Kawasaki,[28] H. R. Khan,[42] H. Kichimi,[8] H. J. Kim,[16] S. K. Kim,[34] S. M. Kim,[35] K. Kinoshita,[4] S. Korpar,[19,13] P. Križan,[18,13] P. Krokovny,[1] S. Kumar,[31] C. C. Kuo,[23] A. Kuzmin,[1] Y.-J. Kwon,[47] J. S. Lange,[5] G. Leder,[11] S. E. Lee,[34] Y.-J. Lee,[25] T. Lesiak,[26] J. Li,[33] S.-W. Lin,[25] D. Liventsev,[12] J. MacNaughton,[11] F. Mandl,[11] T. Matsumoto,[43] A. Matyja,[26] Y. Mikami,[40] W. Mitaroff,[11] K. Miyabayashi,[22] H. Miyake,[30] H. Miyata,[28] R. Mizuk,[12] D. Mohapatra,[46] G. R. Moloney,[20] T. Nagamine,[40] Y. Nagasaka,[9] E. Nakano,[29] M. Nakao,[8] H. Nakazawa,[8] Z. Natkaniec,[26] S. Nishida,[8] O. Nitoh,[44] T. Nozaki,[8] S. Ogawa,[38] T. Ohshima,[21] T. Okabe,[21] S. Okuno,[14] S. L. Olsen,[7] W. Ostrowicz,[26] H. Ozaki,[8] P. Pakhlov,[12] H. Palka,[26] C. W. Park,[35] N. Parslow,[36] L. S. Peak,[36] R. Pestotnik,[13] L. E. Piilonen,[46] N. Root,[1] M. Rozanska,[26] H. Sagawa,[8] Y. Sakai,[8] T. R. Sarangi,[8] N. Sato,[21] T. Schietinger,[17] O. Schneider,[17] J. Schümann,[25] C. Schwanda,[11] A. J. Schwartz,[4] K. Senyo,[21] M. E. Sevior,[20] T. Shibata,[28] H. Shibuya,[38] B. Shwartz,[1] V. Sidorov,[1] J. B. Singh,[31] A. Somov,[4] N. Soni,[31] R. Stamen,[8] S. Stanič,[45,*] M. Starič,[13] K. Sumisawa,[30] T. Sumiyoshi,[43] O. Tajima,[8] F. Takasaki,[8] K. Tamai,[8] N. Tamura,[28] M. Tanaka,[8] Y. Teramoto,[29] X. C. Tian,[32] K. Trabelsi,[7] T. Tsukamoto,[8] S. Uehara,[8] T. Uglov,[12] K. Ueno,[25] S. Uno,[8] P. Urquijo,[20] Y. Ushiroda,[8] G. Varner,[7] K. E. Varvell,[36] S. Villa,[17] C. C. Wang,[25] C. H. Wang,[24] M.-Z. Wang,[25] M. Watanabe,[28] Y. Watanabe,[42] Q. L. Xie,[10] B. D. Yabsley,[46] A. Yamaguchi,[40] Y. Yamashita,[27] M. Yamauchi,[8] Heyoung Yang,[34] J. Ying,[32] J. Zhang,[8] L. M. Zhang,[33] Z. P. Zhang,[33] V. Zhilich,[1] D. Žontar,[18,13] and D. Zürcher[17]

(Belle Collaboration)

[1]*Budker Institute of Nuclear Physics, Novosibirsk*
[2]*Chiba University, Chiba*
[3]*Chonnam National University, Kwangju*
[4]*University of Cincinnati, Cincinnati, Ohio 45221*
[5]*University of Frankfurt, Frankfurt*
[6]*Gyeongsang National University, Chinju*
[7]*University of Hawaii, Honolulu, Hawaii 96822*
[8]*High Energy Accelerator Research Organization (KEK), Tsukuba*
[9]*Hiroshima Institute of Technology, Hiroshima*
[10]*Institute of High Energy Physics, Chinese Academy of Sciences, Beijing*
[11]*Institute of High Energy Physics, Vienna*
[12]*Institute for Theoretical and Experimental Physics, Moscow*
[13]*J. Stefan Institute, Ljubljana*
[14]*Kanagawa University, Yokohama*
[15]*Korea University, Seoul*
[16]*Kyungpook National University, Taegu*
[17]*Swiss Federal Institute of Technology of Lausanne, EPFL, Lausanne*
[18]*University of Ljubljana, Ljubljana*
[19]*University of Maribor, Maribor*
[20]*University of Melbourne, Victoria*
[21]*Nagoya University, Nagoya*
[22]*Nara Women's University, Nara*
[23]*National Central University, Chung-li*
[24]*National United University, Miao Li*
[25]*Department of Physics, National Taiwan University, Taipei*
[26]*H. Niewodniczanski Institute of Nuclear Physics, Krakow*
[27]*Nihon Dental College, Niigata*
[28]*Niigata University, Niigata*

[29]*Osaka City University, Osaka*
[30]*Osaka University, Osaka*
[31]*Punjab University, Chandigarh*
[32]*Peking University, Beijing*
[33]*University of Science and Technology of China, Hefei*
[34]*Seoul National University, Seoul*
[35]*Sungkyunkwan University, Suwon*
[36]*University of Sydney, Sydney NSW*
[37]*Tata Institute of Fundamental Research, Bombay*
[38]*Toho University, Funabashi*
[39]*Tohoku Gakuin University, Tagajo*
[40]*Tohoku University, Sendai*
[41]*Department of Physics, University of Tokyo, Tokyo*
[42]*Tokyo Institute of Technology, Tokyo*
[43]*Tokyo Metropolitan University, Tokyo*
[44]*Tokyo University of Agriculture and Technology, Tokyo*
[45]*University of Tsukuba, Tsukuba*
[46]*Virginia Polytechnic Institute and State University, Blacksburg, Virginia 24061*
[47]*Yonsei University, Seoul*
[48]*Princeton University, Princeton, New Jersey 08545*
(Received 6 March 2005; published 8 June 2005)

We present measurements of decay amplitudes and triple-product correlations in $B \to \phi K^*$ decays based on 253 fb^{-1} of data recorded at the $\Upsilon(4S)$ resonance with the Belle detector at the KEKB e^+e^- storage ring. The decay amplitudes for the three different helicity states are determined from the angular distributions of final-state particles. The longitudinal polarization amplitudes are found to be $0.45 \pm 0.05 \pm 0.02$ for $B^0 \to \phi K^{*0}$ and $0.52 \pm 0.08 \pm 0.03$ for $B^+ \to \phi K^{*+}$ decays. CP- and T-odd CP-violating triple-product asymmetries are measured to be consistent with zero.

DOI: 10.1103/PhysRevLett.94.221804 PACS numbers: 13.25.Hw, 11.30.Er, 12.39.St

The vector-vector $B \to \phi K^*$ decay processes provide clear insights into the underlying $b \to s$ transition by virtue of their clear experimental signatures and relatively unambiguous theoretical interpretation, especially of the many angular correlations that can be formed among the final-state particles. The decays are described by second order penguin diagrams, the first order $b \to s$ transition being forbidden in the standard model (SM). The angular information allows the CP-even and CP-odd states that comprise the $B^0 \to \phi K^{*0}$ decay to be distinguished. Our previous measurement [1] and a recent report by *BABAR* [2] both suggest that the longitudinal polarization component differs from predictions based on the factorization assumption.

In this Letter we report on a further study of this anomaly that is based on a larger data sample and uses observables that are expected to be sensitive to the effects of new physics. We present the first full three-dimensional angular analysis for $B^+ \to \phi K^{*+}$ and an extended study for $B^0 \to \phi K^{*0}$. The decay modes $\phi \to K^+K^-$, $K^{*0} \to K^+\pi^-$, $K^{*+} \to K_S^0\pi^+$, and $K^{*+} \to K^+\pi^0$ are considered. Charge conjugate modes are implied everywhere unless otherwise specified. We report measurements of direct CP asymmetries, triple-product correlations and related T-odd CP-violating asymmetries [3], and other observables that are sensitive to new physics (NP) [4].

This analysis uses a data sample that contains 275×10^6 $B\bar{B}$ pairs collected on the $\Upsilon(4S)$ resonance by the Belle detector [5] at the KEKB e^+e^- collider [6]. The Belle detector is a general purpose magnetic spectrometer equipped with a 1.5 T superconducting solenoid magnet. Charged tracks are reconstructed in a central drift chamber (CDC) and a silicon vertex detector (SVD). Photons and electrons are identified using a CsI(Tl) electromagnetic calorimeter (ECL) located inside the magnet coil. Charged particles are identified using specific ionization (dE/dx) measurements in the CDC as well as information from aerogel Cherenkov counters (ACC) and time of flight counters (TOF).

Event reconstruction is performed as described in Ref. [1]. Candidate B mesons are reconstructed from ϕ and K^* candidates and are identified by the energy difference $\Delta E = E_B^{\rm cms} - E_{\rm beam}^{\rm cms}$, the beam constrained mass $M_{\rm bc} = \sqrt{(E_{\rm beam}^{\rm cms})^2 - (p_B^{\rm cms})^2}$, and K^+K^- invariant mass ($M_{K^+K^-}$), where $E_{\rm beam}^{\rm cms}$ is the beam energy in the center-of-mass (c.m.) system, and $E_B^{\rm cms}$ and $p_B^{\rm cms}$ are the c.m. energy and momentum of the reconstructed B candidate. The B-meson signal region is defined as $M_{\rm bc} > 5.27$ GeV$/c^2$, $|\Delta E| < 45$ MeV, and $|M_{K^+K^-} - M_\phi| < 10$ MeV$/c^2$. The invariant mass of the $K^* \to K\pi$ candidate is required to be less than 70 MeV$/c^2$ from the nominal K^* mass. The signal region is enlarged to

-100 MeV $< \Delta E < 80$ MeV for $B^+ \to \phi K^{*+}(K^{*+} \to K^+\pi^0)$ because of the effects of shower leakage on the ΔE resolution. An additional requirement $\cos\theta_{K^*} < 0.8$ is applied to reduce low momentum π^0 background, where θ_{K^*} is the angle between the direction opposite to the B and the daughter kaon in the rest frame of K^*. These requirements do not affect our results based on a MC study. In the signal region, about 1% of the events have multiple candidates. The candidate with the smallest χ^2 value from B vertex finding and the best π^0 mass in the $K^{*+} \to K^+\pi^0$ decay is used.

The dominant background is $e^+e^- \to q\bar{q}$ ($q = u, d, c, s$) continuum production. Several variables including $S_\perp$ [7], the thrust angle, and the modified Fox-Wolfram moments defined in Ref. [8] are used to exploit the differences between the event shapes for continuum $q\bar{q}$ production (jetlike) and for B decay (spherical) in the c.m. frame of the $\Upsilon(4S)$. These variables are combined into a single likelihood ratio $\mathcal{R}_s = \mathcal{L}_s/(\mathcal{L}_s + \mathcal{L}_{q\bar{q}})$, where $\mathcal{L}_s(\mathcal{L}_{q\bar{q}})$ denotes the signal (continuum) likelihood. The selection requirements on $\mathcal{R}_s$ are determined by maximizing the value of $N_s/\sqrt{N_s + N_b}$ in each B-flavor-tagging quality region [9], where $N_s(N_b)$ represents the expected number of signal (background) events in the signal region.

Backgrounds from other B decay modes such as $B \to K^+K^-K^*$, $B \to f_0(980)K^*(f_0 \to K^+K^-)$, $B \to \phi K\pi$, $B \to K^+K^-K\pi$, and cross feed between the ϕK^* and ϕK decay channels are studied. The contributions from $B \to K^+K^-K^*$ and $B \to f_0K^*$ are estimated from a fit to ΔE, $M_{\rm bc}$, and $M_{K^+K^-}$ distributions. The $M_{K^+K^-}$ distribution for $B \to K^+K^-K^*$ is determined from Monte Carlo (MC) simulations. The $f_0(980)$ line shape is obtained from MC, where an S-wave Breit-Wigner with a 61 MeV$/c^2$ intrinsic width [10] is assumed. The uncertainty in the $f_0(980)$ width (40–100 MeV$/c^2$) [11] is taken as a source of systematic error. The contributions from $B \to K^+K^-K^*(B \to f_0K^*)$ are estimated together with the ϕK^* signal and are found to be 1% to 7% (1% to 3%) [12] of the signal yield. The background from $B \to \phi K\pi$ decays is evaluated with fits to the $K\pi$ invariant mass and is found to be about 1%. The contamination from four-body $B \to K^+K^-K\pi$ decays is checked by performing fits to the events in the $\phi \to K^+K^-$ and $K^* \to K\pi$ mass sidebands and is found to be less than 1%. To remove the contamination from ϕK decays, these decays are explicitly reconstructed and rejected.

TABLE I. Number of events observed in the signal region ($N_{\rm ev}$), signal yields (N_s), and the direct CP asymmetries (A_{CP}) obtained in the fits, with statistical and systematic uncertainties.

Mode	$N_{\rm ev}$	N_s	A_{CP}
ϕK^{*0}	309	173 ± 16	$0.02 \pm 0.09 \pm 0.02$
ϕK^{*+}	173	85^{+12}_{-11}	$-0.02 \pm 0.14 \pm 0.03$
$K^{*+}(K_S^0\pi^+)$	76	$37.9^{+7.7}_{-7.0}$	$-0.14 \pm 0.21 \pm 0.04$
$K^{*+}(K^+\pi^0)$	97	$47.3^{+9.1}_{-8.1}$	$0.09 \pm 0.19 \pm 0.04$

The signal yields (N_s) are extracted by extended unbinned maximum-likelihood fits performed simultaneously to the ΔE, $M_{\rm bc}$, and $M_{K^+K^-}$ distributions. Reconstructed B candidates with $|\Delta E| < 0.25$ GeV, $M_{\rm bc} > 5.2$ GeV$/c^2$, and $M_{K^+K^-} < 1.07$ GeV$/c^2$ are included in the fits. The signal probability density functions (PDFs) are a single Gaussian in $M_{\rm bc}$, a core Gaussian plus a bifurcated Gaussian (Gaussian with different widths on either side of the mean) as the tail in the ΔE distribution, and a Breit-Wigner shape in $M_{K^+K^-}$. The means and widths of ΔE and $M_{\rm bc}$ are verified using $B \to J/\psi K^*$ decays. The mean and width of the ϕ mass peak are determined using an inclusive $\phi \to K^+K^-$ data sample.

The PDF shapes for the continuum events are parametrized by an ARGUS function [13] in $M_{\rm bc}$, a linear function in ΔE, and a sum of a threshold function and a Breit-Wigner function in $M_{K^+K^-}$. The parameters of the functions are determined by a fit to the events in the sideband. The signal and background yields are allowed to float in the fit while other PDF parameters are fixed. The direct CP asymmetries, $A_{CP} = \frac{N(\bar{B}\to\bar{f})-N(B\to f)}{N(\bar{B}\to\bar{f})+N(B\to f)}$, are also studied. The measured signal yields and direct CP asymmetries are summarized in Table I. The distributions of ΔE, $M_{\rm bc}$, and $M_{K^+K^-}$ are shown in Fig. 1.

The decay angles of a B-meson decaying to two vector mesons ϕ and K^* are defined in the transversity basis [14]. The x-y plane is defined to be the decay plane of K^* and the x axis is in the direction of the ϕ meson. The y axis is perpendicular to the x axis in the decay plane and is on the same side as the kaon from the K^* decay. The z axis is perpendicular to the x-y plane according to the right-hand rule, $\theta_{\rm tr}$ ($\phi_{\rm tr}$) is the polar (azimuthal) angle with respect to the z axis of the K^+ from ϕ decay in the ϕ rest frame, and θ_{K^*} is defined earlier.

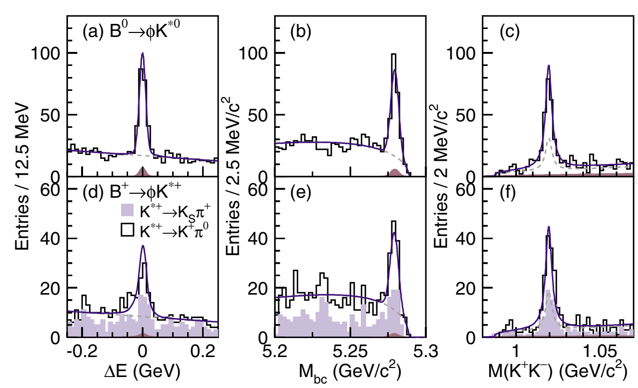

FIG. 1 (color online). Distributions of the ΔE, $M_{\rm bc}$, and $M_{K^+K^-}$ for $B^0 \to \phi K^{*0}$ (a), (b), (c), and for $B^+ \to \phi K^{*+}$ (d), (e), (f), with other variables in signal region. Solid curves show the fit results. The continuum background components are shown by the dashed curves. The dark shaded areas represent the contributions from $B \to K^+K^-K^*$ and $B \to f_0K^*$ decays.

The distribution of the angles, θ_{K^*}, $\theta_{\rm tr}$, and $\phi_{\rm tr}$ is given by [15]

$$\frac{d^3R_{\phi K^*}(\phi_{\rm tr},\cos\theta_{\rm tr},\cos\theta_{K^*})}{d\phi_{\rm tr}d\cos\theta_{\rm tr}d\cos\theta_{K^*}} = \frac{9}{32\pi}[|A_\perp|^2 2\cos^2\theta_{\rm tr}\sin^2\theta_{K^*} + |A_\parallel|^2 2\sin^2\theta_{\rm tr}\sin^2\phi_{\rm tr}\sin^2\theta_{K^*} + |A_0|^2 4\sin^2\theta_{\rm tr}\cos^2\phi_{\rm tr}\cos^2\theta_{K^*} + \sqrt{2}{\rm Re}(A_\parallel^* A_0)\sin^2\theta_{\rm tr}\sin 2\phi_{\rm tr}\sin 2\theta_{K^*} - \eta\sqrt{2}{\rm Im}(A_0^* A_\perp)\sin 2\theta_{\rm tr}\cos\phi_{\rm tr}\sin 2\theta_{K^*} - 2\eta{\rm Im}(A_\parallel^* A_\perp)\sin 2\theta_{\rm tr}\sin\phi_{\rm tr}\sin^2\theta_{K^*}], \tag{1}$$

where A_0, $A_\parallel$, and $A_\perp$ are the complex amplitudes of the three helicity states in the transversity basis with the normalization condition $|A_0|^2 + |A_\parallel|^2 + |A_\perp|^2 = 1$, and $\eta = +1(-1)$ corresponds to $B(\bar{B})$ mesons and is determined from the charge of the kaon or pion in the K^* decay. The longitudinal polarization component is denoted by A_0; $A_\perp(A_\parallel)$ is the transverse polarization along the z axis (y axis). The value of $|A_\perp|^2(|A_0|^2 + |A_\parallel|^2)$ is the CP-odd (CP-even) fraction in the decay $B \to \phi K^{*0}$ [15]. The presence of final-state interactions (FSI) results in phases that differ from either 0 or $\pm\pi$.

The complex amplitudes are determined by performing an unbinned maximum-likelihood fit to the $B \to \phi K^*$ candidates in the signal region. The combined likelihood is given by

$$\mathcal{L} = \prod_i^{N_{\rm ev}} \epsilon(\phi_{\rm tr},\cos\theta_{\rm tr},\cos\theta_{K^*})\sum_j f_j R_j(\phi_{\rm tr},\cos\theta_{\rm tr},\cos\theta_{K^*}), \tag{2}$$

where j denotes the contributions from ϕK^*, $q\bar{q}$, $K^+K^-K^*$, and f_0K^*; R_j is the angular distribution function (ADF). The ADF $R_{q\bar{q}}$ is determined from sideband data, and $R_{K^+K^-K^*}$ from events with 1.04 GeV$/c^2 < M_{K^+K^-} <$ 1.075 GeV$/c^2$; $R_{f_0K^*}$ is obtained from $B \to f_0K^*$ MC events. The detection efficiency (ϵ) is determined using MC simulations assuming a phase space decay. The fractions f_j are parametrized as a function of ΔE, $M_{\rm bc}$, and $M_{K^+K^-}$. The value of arg(A_0) is set to zero and $|A_\parallel|^2$ is calculated from the normalization condition. The four parameters [$|A_0|^2$, $|A_\perp|^2$, arg$(A_\parallel)$, and arg$(A_\perp)$] are determined from the fit. There is a twofold ambiguity in the solutions for the phases; the chosen set of solutions is the one suggested in Ref. [16]. Figure 2 shows the angular distributions with projections of the fit superimposed. The obtained amplitudes are summarized in Table II.

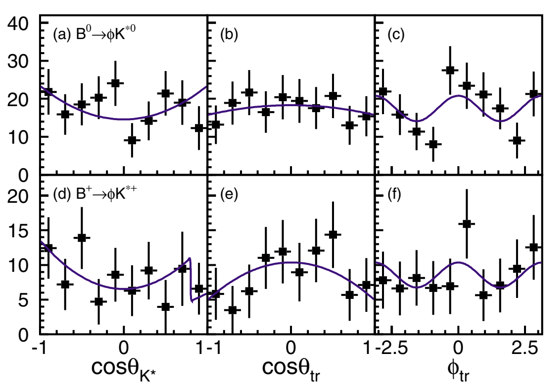

FIG. 2 (color online). Projected distributions of the three transversity angles for $B^0 \to \phi K^{*0}$ (a), (b), (c), and for $B^+ \to \phi K^{*+}$ (d), (e), (f). Solid lines show the fit results. The points with error bars show the efficiency corrected data after background subtraction. The two K^{*+} decay modes are combined in (d), (e), (f). The discontinuity in (d) is due to the requirement of $\cos\theta_{K^*} <$ 0.8 in $B^+ \to \phi K^{*+}(K^{*+} \to K^+\pi^0)$.

The systematic uncertainties on the amplitudes are dominated by the efficiency modeling (4%–5%), continuum background (3–4%), slow pion efficiency (2%–3%), and $K^+K^-K^*$ ADF (1%–2%). The remaining possible systematic errors, such as the angular resolution, signal yields, background from higher K^* states, and width of the f_0, are estimated to be less than 1%.

The triple product for a B meson decay to two vector mesons takes the form $\vec{q}\cdot(\vec{\epsilon}_1 \times \vec{\epsilon}_2)$, where $\vec{q}$ is the momentum of one of the vector mesons, and $\vec{\epsilon}_1$ and $\vec{\epsilon}_2$ are the polarizations of the two vector mesons. The following two T-odd [3,17] quantities

$$A_T^0 = {\rm Im}(A_\perp A_0^*), \qquad A_T^\parallel = {\rm Im}(A_\perp A_\parallel^*), \tag{3}$$

provide information on the asymmetry of the triple products. The SM predicts very small values for A_T^0 and $A_T^\parallel$. The comparison of these triple-product asymmetries (A_T^0 and $A_T^\parallel$) with the corresponding quantities for the CP-conjugate decays ($\bar{A}_T^0$ and $\bar{A}_T^\parallel$) provides an observable sensitive to T-odd CP violation.

Additional variables that can be accessed by angular analyses are suggested in Ref. [4] and are given by

TABLE II. The decay amplitudes obtained for $B^0 \to \phi K^{*0}$ and $B^+ \to \phi K^{*+}$. The first uncertainties are statistical and the second are systematic.

Mode	ϕK^{*0}	ϕK^{*+}
$\lvert A_0\rvert^2$	$0.45 \pm 0.05 \pm 0.02$	$0.52 \pm 0.08 \pm 0.03$
$\lvert A_\perp\rvert^2$	$0.30 \pm 0.06 \pm 0.02$	$0.19 \pm 0.08 \pm 0.02$
arg$(A_\parallel)$ (rad)	$2.39 \pm 0.24 \pm 0.04$	$2.10 \pm 0.28 \pm 0.04$
arg$(A_\perp)$ (rad)	$2.51 \pm 0.23 \pm 0.04$	$2.31 \pm 0.30 \pm 0.07$

TABLE III. The measured decay amplitudes and triple-product correlations in the B^0 and $\bar{B}^0$ samples.

Mode	B^0	$\bar{B}^0$
$\lvert A_0\rvert^2$	$0.39 \pm 0.08 \pm 0.03$	$0.51 \pm 0.07 \pm 0.02$
$\lvert A_\perp\rvert^2$	$0.37 \pm 0.09 \pm 0.02$	$0.25 \pm 0.07 \pm 0.01$
$\arg(A_\parallel)$ (rad)	$2.72^{+0.46}_{-0.38} \pm 0.14$	$2.08 \pm 0.31 \pm 0.04$
$\arg(A_\perp)$ (rad)	$2.81 \pm 0.36 \pm 0.11$	$2.22 \pm 0.35 \pm 0.05$
A_T^0	$0.13^{+0.11}_{-0.14} \pm 0.04$	$0.28 \pm 0.08 \pm 0.01$
$A_T^\parallel$	$0.03 \pm 0.08 \pm 0.01$	$0.03 \pm 0.06 \pm 0.01$

$$\Lambda_{\perp i} = -\mathrm{Im}(A_\perp A_i^* - \bar{A}_\perp \bar{A}_i^*), \quad \Lambda_{\parallel 0} = \mathrm{Re}(A_\parallel A_0^* + \bar{A}_\parallel \bar{A}_0^*),$$
$$\Sigma_{\perp i} = -\mathrm{Im}(A_\perp A_i^* + \bar{A}_\perp \bar{A}_i^*), \quad \Sigma_{\parallel 0} = \mathrm{Re}(A_\parallel A_0^* - \bar{A}_\parallel \bar{A}_0^*),$$
$$\Lambda_{\lambda\lambda} = \frac{1}{2}(|A_\lambda|^2 + |\bar{A}_\lambda|^2), \quad \Sigma_{\lambda\lambda} = \frac{1}{2}(|A_\lambda|^2 - |\bar{A}_\lambda|^2), \tag{4}$$

where the subscript λ is either 0, $\parallel$, or $\perp$, and i is 0 or $\parallel$. The variables $\Lambda_{\perp 0}$ and $\Lambda_{\perp\parallel}$ are sensitive to T-odd CP-violating new physics. The following equations should hold in the absence of NP:

$$\Sigma_{\lambda\lambda} = 0, \qquad \Sigma_{\parallel 0} = 0, \qquad \Lambda_{\perp i} = 0. \tag{5}$$

By separating B^0 and $\bar{B}^0$ samples and rearranging fitting parameters in the unbinned maximum-likelihood fit, we measured the decay amplitudes for the B^0 and $\bar{B}^0$, the triple-product correlations, and the other NP-sensitive observables as given in Tables III and IV. The T-odd CP-violating variables $\Lambda_{\perp 0}$ and $\Lambda_{\perp\parallel}$ are measured to be $0.16^{+0.16}_{-0.14} \pm 0.03$ and $0.01 \pm 0.10 \pm 0.02$, respectively, consistent with the SM predictions.

In summary, improved measurements of the decay amplitudes for $B \to \phi K^*$, based on fits to angular distributions in the transversity basis, are presented. The results are consistent with our previous measurements [1] with improved precision. The measured value of $|A_\perp|^2$ shows that CP-odd ($|A_\perp|^2$) and CP-even ($|A_0|^2 + |A_\parallel|^2$) components are present in ϕK^* decays in a ratio of about 1:2. Phases of both $A_\perp$ and $A_\parallel$ differ from zero or $-\pi$ by 4.3 standard deviations (σ), which provides evidence for the presence of final-state interactions. The measured direct CP asymmetries in these modes are consistent with zero; the corresponding 90% confidence level limits are $-0.14 < A_{CP}(\phi K^{*0}(K^+\pi^-)) < 0.17$ and $-0.25 < A_{CP}(\phi K^{*+}) < 0.22$. Measurements of the T-odd CP-violation sensitive differences between triple-product asymmetries, $A_T^0 - \bar{A}_T^0$, and $A_T^\parallel - \bar{A}_T^\parallel$, indicate no significant deviations from zero, consistent with *BABAR* measurements [2]. Our data show no significant deviations from the expectations: $\Sigma_{\lambda\lambda} = 0$, $\Sigma_{\parallel 0} = 0$, and $\Lambda_{\perp i} = 0$, indicating no evidence for new physics.

TABLE IV. Λ and Σ values obtained from the decay amplitudes measured for B^0 and $\bar{B}^0$ separately.

$\Lambda_{00} = 0.45 \pm 0.05 \pm 0.02$	$\Sigma_{00} = -0.06 \pm 0.05 \pm 0.01$
$\Lambda_{\parallel\parallel} = 0.24 \pm 0.06 \pm 0.02$	$\Sigma_{\parallel\parallel} = -0.01 \pm 0.06 \pm 0.01$
$\Lambda_{\perp\perp} = 0.31 \pm 0.06 \pm 0.01$	$\Sigma_{\perp\perp} = 0.06 \pm 0.05 \pm 0.01$
$\Sigma_{\perp 0} = -0.41^{+0.16}_{-0.14} \pm 0.04$	$\Lambda_{\perp 0} = 0.16^{+0.16}_{-0.14} \pm 0.03$
$\Sigma_{\perp\parallel} = -0.06 \pm 0.10 \pm 0.01$	$\Lambda_{\perp\parallel} = 0.01 \pm 0.10 \pm 0.02$
$\Lambda_{\parallel 0} = -0.45 \pm 0.11 \pm 0.01$	$\Sigma_{\parallel 0} = -0.11 \pm 0.11 \pm 0.02$

We thank the KEKB group for the excellent operation of the accelerator, the KEK cryogenics group for the efficient operation of the solenoid, and the KEK computer group and the NII for valuable computing and Super-SINET network support. We acknowledge support from MEXT and JSPS (Japan); ARC and DEST (Australia); NSFC (Contract No. 10175071, China); DST (India); the BK21 program of MOEHRD and the CHEP SRC program of KOSEF (Korea); KBN (Contract No. 2P03B 01324, Poland); MIST (Russia); MHEST (Slovenia); SNSF (Switzerland); NSC and MOE (Taiwan); and DOE (USA).

*On leave from Nova Gorica Polytechnic, Nova Gorica.

[1] K.-F. Chen *et al.* (Belle Collaboration), Phys. Rev. Lett. **91**, 201801 (2003).
[2] B. Aubert *et al.* (BABAR Collaboration), Phys. Rev. Lett. **93**, 231804 (2004); Phys. Rev. Lett. **91**, 171802 (2003).
[3] A. Datta and D. London, Int. J. Mod. Phys. A **19**, 2505 (2004).
[4] D. London, N. Sinha, and R. Sinha, Phys. Rev. D **69**, 114013 (2004).
[5] A. Abashian *et al.*, Nucl. Instrum. Methods Phys. Res., Sect. A **479**, 117 (2002).
[6] S. Kurokawa and E. Kikutani, Nucl. Instrum. Methods Phys. Res., Sect. A **499**, 1 (2003).
[7] R. Ammar *et al.* (CLEO Collaboration), Phys. Rev. Lett. **71**, 674 (1993).
[8] K. Abe *et al.* (Belle Collaboration), Phys. Lett. B **517**, 309 (2001).
[9] H. Kakuno *et al.*, Nucl. Instrum. Methods Phys. Res., Sect. A **533**, 516 (2004).
[10] A. Garmash *et al.* (Belle Collaboration), hep-ex/0412066.
[11] S. Eidelman *et al.*, Phys. Lett. B **592**, 1 (2004).
[12] The range corresponds to the range of values for different submodes. This convention is used throughout this Letter.
[13] The functional form is $x\sqrt{1-x^2}\exp[\alpha(1-x^2)]$, where $x = M_{\mathrm{bc}}/E_{\mathrm{beam}}$. H. Albrecht *et al.* (ARGUS Collaboration), Phys. Lett. B **241**, 278 (1990); Phys. Lett. B**254**, 288 (1991).
[14] I. Dunietz *et al.*, Phys. Rev. D **43**, 2193 (1991).
[15] K. Abe, M. Satpathy, and H. Yamamoto, hep-ex/0103002.
[16] M. Suzuki, Phys. Rev. D **64**, 117503 (2001).
[17] We take the definitions of $A_T^0 = A_T^{(1)}$ and $A_T^\parallel = A_T^{(2)}$, but $\bar{A}_T^0 = -\bar{A}_T^{(1)}$ and $\bar{A}_T^\parallel = -\bar{A}_T^{(2)}$. The variables $A_T^{(1)}$ and $A_T^{(2)}$ are defined in Ref. [3].